Geophysical Response of Saturated Rock Joints during Shear



Han, K.

Lyles School of Civil Engineering, Purdue University, West Lafayette, IN, USA

Pyrak-Nolte, L. J.

Department of Physics, Department of Earth and Atmospheric Sciences, Lyles School of Civil Engineering, Purdue University, West Lafayette, IN, USA

Bobet, A.

Lyles School of Civil Engineering, Purdue University, West Lafayette, IN, USA

Copyright 2022 ARMA, American Rock Mechanics Association

This paper was prepared for presentation at the 56th US Rock Mechanics/Geomechanics Symposium held in Santa Fe, New Mexico, USA, 26-29 June 2022. This paper was selected for presentation at the symposium by an ARMA Technical Program Committee based on a technical and critical review of the paper by a minimum of two technical reviewers. The material, as presented, does not necessarily reflect any position of ARMA, its officers, or members. Electronic reproduction, distribution, or storage of any part of this paper for commercial purposes without the written consent of ARMA is prohibited. Permission to reproduce in print is restricted to an abstract of not more than 200 words; illustrations may not be copied. The abstract must contain conspicuous acknowledgement of where and by whom the paper was presented.

ABSTRACT: Monitoring the frictional behavior of rock discontinuities is essential for the identification of potential natural hazards caused by mechanical instability. Active seismic monitoring of changes in transmitted and/or reflected compressional (P) and shear (S) waves has been used as a non-destructive method to assess the degree of damage inside rock and to monitor slip along a discontinuity. The objective of this study is to explore the geophysical response of a saturated rock joint undergoing shear. Laboratory shear tests are conducted on prismatic Indiana limestone specimens. Induced tension fractures resulted in specimens composed of two blocks (152.4 mm × 127.0 mm × 50.8 mm) with rough contact surfaces. Direct shear experiments were performed inside a metal confinement chamber under an effective normal stress of 2 MPa on water-saturated specimens. During the experiments, the chamber pressure, the total normal load, the shear load and the slip displacement were monitored. During the tests, continuous pulses of P-and S-waves were transmitted through the specimen and the amplitudes of the transmitted and reflected waves were recorded. The paper provides results of the mechanical and geophysical response of saturated joints and compares them with those obtained from similar, but dry, joints. For dry joints, both transmitted and reflected P- and S-waves show a distinct peak wave amplitude prior to shear failure. However, for saturated joints, a distinct peak in amplitude is only observed in both transmitted and reflected S-waves. Transmitted and reflected P-waves, propagated through saturated rock, displayed a continuous decrease and increase in amplitude, respectively, but had a sudden change in the rate of amplitude change that can be taken as a seismic precursor to joint shear failure.

1. INTRODUCTION

The stability of a rock mass depends on the presence of pre-existing discontinuities, such as fractures, joints, and faults, and on their response to changes in stress, pressure, fluids and geochemical conditions. The ability to evaluate and assess the mechanical stability and frictional behavior of rock joints has been considered a longstanding goal for the design of geotechnical structures and prevent potential natural hazards. Active seismic monitoring is a nondestructive method to probe inside rock to detect fractures and to monitor their evolution with changes in stress, as well as the degree of damage over time. Changes in transmitted and reflected compressional (P) and shear (S) waves have been used as seismic precursors to shear failure of rock joints (Hedayat et al., 2014a, 2014b, 2018; El Fil et al., 2019, 2021). Recent laboratory experiments have shown that converted waves (S to P & P to S) may be used to track the mechanical behavior of rock joints and detect precursors to shear failure (Nakagawa et al., 2000; El Fil et al., 2021, Gheibi et al, 2021).

However, most previous experiments had been performed on dry rock joints. Yet, in the field, rock discontinuities are often found below the water table. This situation poses additional challenges because the presence of water affects not only the mechanical behavior of a rock joint (Barton, 1976), but also the joint's geophysical signature (Pyrak-Nolte et al., 1990, 2006; Choi, 2013). Thus, it is necessary to explore how fluid saturation affects geophysical signatures and whether wave propagation can still be used to monitor the mechanical behavior of rock joints under saturated conditions.

The objective of this study is to explore the geophysical response of saturated rock joints undergoing shear. Vacuum saturation and fluid back pressure were used to achieve full saturation of a rock specimen. Direct shear tests were performed on tensile-fractured rock joints, with well-mated rough surfaces, placed in a custom-made pressure chamber. This study explores changes in transmitted and reflected P- and S-waves during shear. In

addition, results from saturated rock joints are compared with those from dry joints.

2. METHODOLOGY

2.1 Specimen Geometry and Preparation

Tension-fractured Indiana limestone joints were prepared to simulate a natural rock discontinuity and to explore the geophysical response of rock joints during shear. The mechanical and geophysical properties of Indiana limestone used for the experiments are summarized in Table 1 (Modiriasari et al., 2017; Han et al., 2021).

Table 1. Mechanical and geophysical properties of Indiana limestone.

Properties	Value
Density, ρ (g/cm ³)	2.29
Porosity, n (%)	14
UCS (MPa)	47
Young's modulus, E (GPa)	7.4
P-wave velocity, V _p (m/s)	4,380
S-wave velocity, V _s (m/s)	2,570

Limestone blocks, with dimensions of $152.4 \text{ mm} \times 127.0 \text{ mm} \times 50.8 \text{ mm}$ (6 in \times 5 in \times 2 in), were collected from Bedford, Indiana. The blocks were fractured using the Brazilian technique (Jager and Cook, 1979) or split cylinder method (ASTM D3967) to obtain well-mated joint surfaces (Fig. 1). A small notch along the sides of the specimen, with a depth of 0.508 mm (0.2 in), was made with a saw to facilitate splitting of the block during loading. Hence, the net area of the joint surface was $142.24 \text{ mm} \times 116.84 \text{ mm}$ (5.6 in \times 4.6 in).



Fig. 1. Indiana limestone joint specimen with a tensile-fractured rough surface.

The surface roughness of the rock joint, prior to shear, was measured using a laser profilometer, along the shear direction. A Keyence LK-G152 Laser (120 μ m spot size) was used to scan the surface roughness of the specimen, with a step size of 250 μ m, which was placed on a motion-controlled (Newport MTM250PP1) translation stage. The

probability distribution of asperity heights of the rock joint is shown in Fig. 2. The distribution represents a maximum height of 672 μ m and a minimum height of 613 μ m, with a standard deviation of 225 μ m.

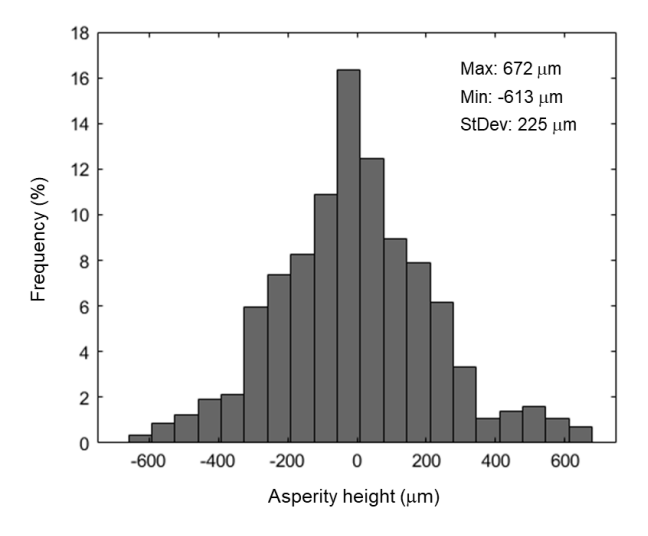


Fig. 2. Frequency distribution of asperity height.

The jointed rock specimen was fully saturated to investigate the effects of saturation on the joint's geophysical signature. It is well-known that an increase in back pressure (pore fluid pressure) compresses the air bubbles that may be trapped in the rock matrix and dissolve them into the pore fluid. Rock saturation is thought be achieved when the Skempton's B-value coefficient becomes independent of back pressure. Three cylindrical Indiana limestone specimens, obtained from the same quarry, were used to determine the magnitude of the back pressure required for full saturation. Saturation was achieved through a two-step process: (1) vacuum saturation of the rock for 24 hours; (2) increase the back pressure until constant B-value. The experimental results showed that, at back pressures greater than $3.2 \sim 3.6$ MPa, the B-value did not change with an additional increase in back pressure, thus indicating that full saturation was reached (Han et al., 2021). The B-values, at full saturation, were $0.79 \sim 0.86$, which are consistent with those reported by others, e.g., Mesri et al. (1976). To ensure full saturation, a pore pressure of 4 MPa was used for all the shear tests on Indiana limestone specimens.

2.2 Experimental Setup

A water-pressurized chamber and a biaxial compression frame were designed and built to conduct direct shear tests on dry and saturated rock joints. Schematic drawings of the chamber and the shear testing apparatus are shown in Fig. 3. The front and back faces have bolt connections and O-rings for a seal. The shear testing apparatus is placed inside the chamber. The loading shafts and their seals are placed at the top- and right-sides of the chamber. One of the shafts is used to impose the vertical/shear load and the other, the horizontal/confinement load. The chamber has

four orifices. Two of those are used to apply the back pressure to the specimen and the chamber pressure; the other two, for cable feedthrough.

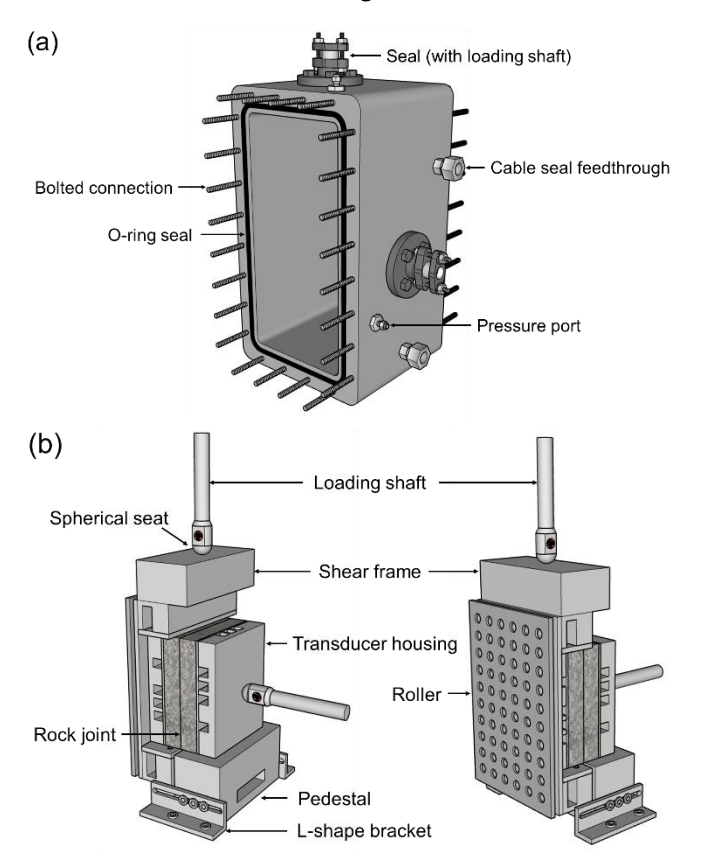


Fig. 3. Schematic drawings of equipment: (a) water-pressurized chamber; (b) direct shear testing apparatus, inside the chamber.

The complete experimental setup is shown in Fig. 4. Fig. 4 shows the water-pressurized chamber and the horizontal loading frame placed on the platform of a conventional loading machine. The rock specimen is placed inside the water-pressurized chamber, where it is loaded in shear/biaxial compression. The horizontal loading frame applies, through the horizontal shaft, the normal stress to the specimen, while the shear is imposed by the conventional loading machine, through the vertical shaft. The horizontal load is applied by a flat-jack that is computer-controlled, while the load is supported by a reaction frame.

During the experiments, the chamber pressure, the total normal load, the shear load and the slip displacement were monitored. The loads were obtained from strain gauges, attached to the tips of the loading shafts, placed inside the chamber to measure the actual load imposed and thus exclude any friction that may develop between the chamber seals and the shafts. The displacements were measured by an external LVDT.

Ultrasonic transducers were housed inside the loading platens, as shown in Fig. 4. Ultrasonic transducers, V103-RM and V153-RM (Olympus Panametrics) with a central frequency of 1 MHz were employed for the tests. These

piezoelectric transducers have been successfully used for compressional (P) and shear (S) wave propagation in previous studies (Li et al., 2009; Choi et al., 2014; Hedayat et al., 2014, 2018; El Fil et al., 2019, 2021). Two transducer arrays (source and receiver), with a total of 10 pairs of transducers, were used to generate seismic waves and capture both transmitted and reflected waves. There were four pairs of P-wave transducers (3P, 4P, 5P, and 9P) and six pairs of S-wave transducers (1S, 2S, 6S, 7S, 8S, and 10S). All shear wave transducers were oriented to align the polarizations perpendicular to the shear direction.

A pulser-receiver (Olympus Panametrics model 5077PR) was employed to generate 400 V square wave pulses, with a repetition rate of 1 kHz, to the source transducers. The data acquisition system enabled a synced ultrasonic wave measurement. The system consisted of a chassis (PXI-1042), with two multiplexer terminal blocks (TB-2630), a 68-pin terminal block (TB-2706), and a two channel 14-bit 100 MHz digitizer (PXI-5122), to record multiple transmitted and reflected full waveforms and to switch between source and receiver transducers.

The procedure for the direct shear tests involved the following steps:

- (a) A tension-fractured limestone specimen was prepared. For dry conditions, the specimen was oven-dried at 40°C for 24 hours, to remove any residual moisture. For saturated conditions, the specimen was vacuum-saturated for 24 hours to reduce any air bubbles trapped in the pores of the rock. Deionized water was used as the pore fluid, to minimize any chemical reaction with the rock specimen.
- (b) The rock joint specimen was placed inside the chamber. The desired effective normal stress was applied first to the rock specimen and was held constant for the duration of the test. In this study, an effective normal stress of 2 MPa was used (i.e., confining pressure 6 MPa and pore pressure 4 MPa). For dry conditions, the seismic wave transducers were coupled to the specimen using baked honey (dried at 90°C for 90 minutes).
- (c) To fully saturate the specimen, the chamber pressure was increased until reaching the magnitude determined from the B-value tests. To do this, the total normal stress and chamber pressure were incrementally increased, while keeping the effective normal stress constant, until the chamber pressure reached the desired value (4 MPa in this study).
- (d) The shear load was applied by imposing a constant displacement rate of 8 μ m/s. An electronic feedback-loop controller adjusted the pressure of the hydraulic flat jack to keep the normal stress constant during shearing even when the joint dilated from slip.

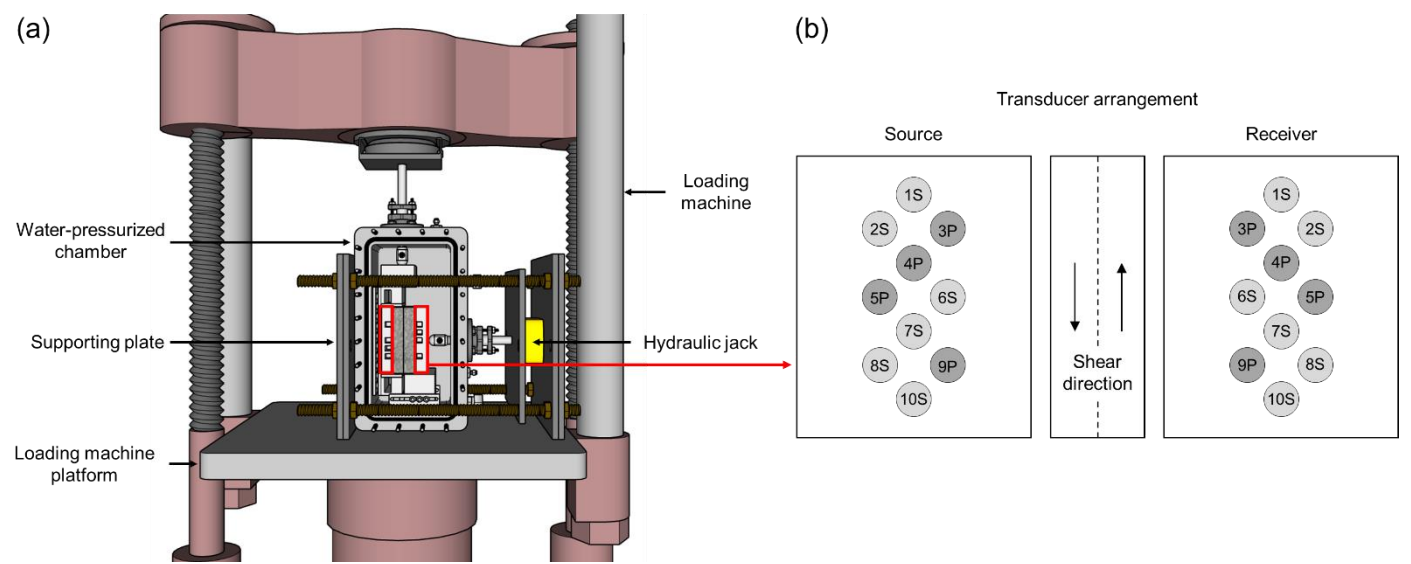


Fig. 4. Experimental set-up for direct shear tests: (a) Overall setup; (b) transducer arrangement inside loading platens.

(e) The vertical and horizontal loads, as well as the displacements were measured using the strain gauges attached to the tips of the loading shafts and the LVDTs, respectively. During the tests, seismic waves were transmitted across the rock specimen and recorded with a sampling rate of 100 MHz to yield a 0.01 μs/point resolution. Transmitted, reflected and converted waves were recorded every second until the test was completed. A data acquisition system was used to capture and store all measurements simultaneously.

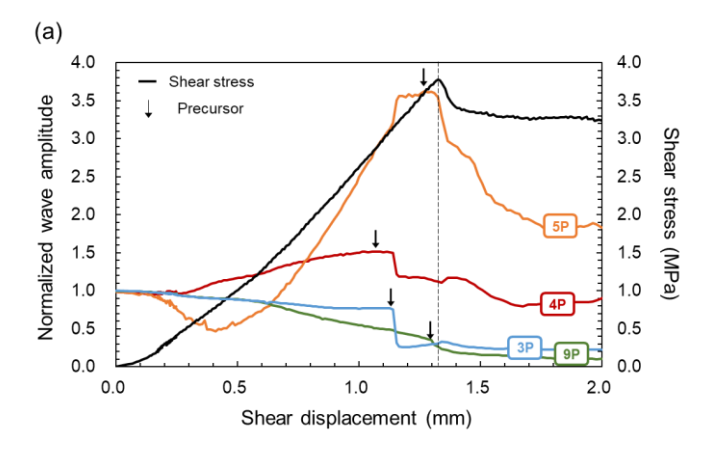
3. RESULTS AND DISCUSSION

Direct shear experiments were conducted on dry and saturated Indiana limestone specimens, at an effective normal stress of 2 MPa. Seismic wave amplitudes were obtained by using a wavelet analysis and plotting the peak amplitudes at each transducer's dominant frequency. Afterwards, the obtained amplitudes were normalized with respect to the initial value prior to shear. Results from transducer 8S were not available because the transducer had very weak signals.

3.1. Dry Joints

The representative shear stress — shear displacement behavior for a dry specimen, along with the normalized transmitted wave amplitudes, is shown in Fig. 5. After the initial seating deformations of the specimen (Fig. 5), the shear stress increased with increasing shear displacement until it reached the peak shear strength of the joint. Then, the shear stress decreased and approached a steady-state value (residual shear strength). The figure also shows that the amplitudes of the transmitted P- and S-waves increased as the shear stress increased. For most transducers, a maximum in the transmitted wave amplitude occurred prior to the peak shear strength. Afterwards, the amplitude quickly decreased. Peaks in the normalized amplitude of the transmitted wave occurred prior to the peak shear strength, which are considered as

seismic precursors to shear failure of the rock joint (Hedayat et al., 2014a, 2014b).



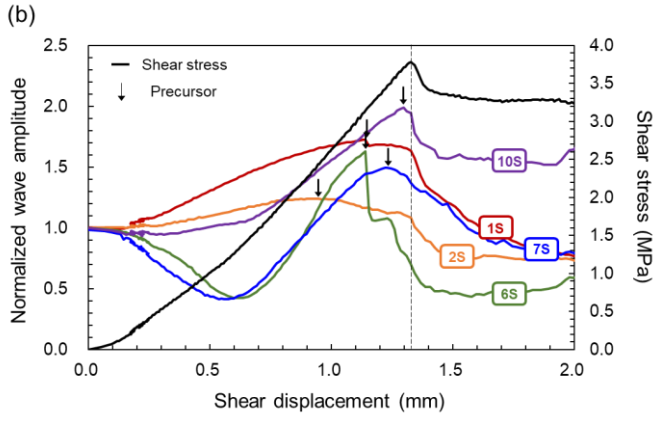
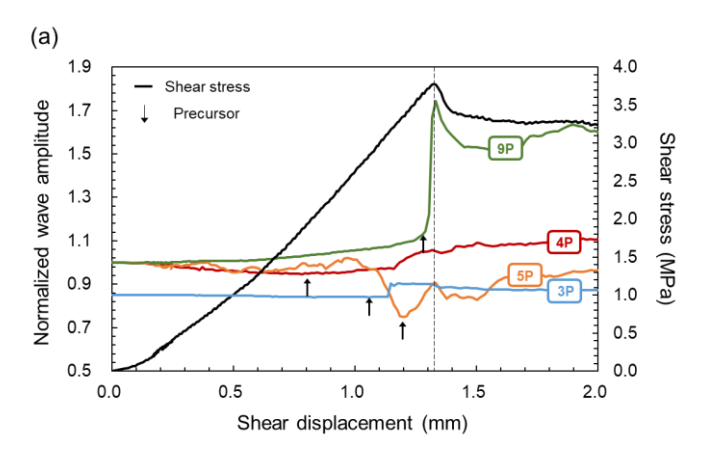


Fig. 5. Transmitted wave amplitude through a rock joint under dry conditions: (a) P-waves; (b) S-waves.

In Fig. 5, seismic precursors (black arrows) and shear failure (dashed vertical line) are shown. Based on the transmitted wave response, in the initial stages of the test, an increase in transmission is observed because of an increase in the contact area and interlocking of the asperities between the two fracture surfaces. The peak of transmission and subsequent decrease in amplitude

denote the onset of local damage of those asperities sampled by the transmitted wave, which is associated with a decrease in the local stiffness of the joint. Thus, a reduction in transmitted amplitude prior the peak shear stress indicates that asperity contacts begin to fail for a dry joint. Hence, a maximum in transmitted wave amplitude can be considered as a precursor to the shear failure of the rock joint. After the peak shear stress (macroscopic shear failure), the transmitted wave amplitude decreases. Scuderi et al. (2016) observed a similar behavior during stick-slip events observed in quartz powder, used to simulate fault gouge material. In addition, Hedayat et al. (2018) and El Fil et al. (2019, 2021) also found a similar geophysical response from both natural and artificial rock joints under dry conditions.

The reflected wave amplitudes are shown in Fig. 6, together with the shear stress – shear displacement for the same dry joint. In contrast to the transmitted waves, the reflected wave amplitudes decreased in amplitude with increasing shear stress, as the contact area of interface increased. The reflected wave amplitudes were observed to reach a minimum prior to the peak shear strength. During the post-peak stage, the reflected wave amplitude increased as the damage on the interface caused a loss of contact area between the two joint surfaces. This behavior is expected and is consistent with measurements of the transmitted waves. Consequently, a minimum in the amplitude of reflected waves can be also viewed as a precursor to the failure of a rock joint. Note that the precursors from the reflection mode occurred first, followed by those from the transmission mode (compare Fig. 5 with Fig. 6), which is consistent with a similar observation reported by El Fil et al. (2021). For example, for transducer 6S, the precursor from the transmitted signals emerges at a shear displacement of 1.14 mm, while that from reflected signals occurs at a shear displacement of 1.08 mm. Those results may indicate that the reflection mode is more sensitive to the damage on the asperities of the rock surface.



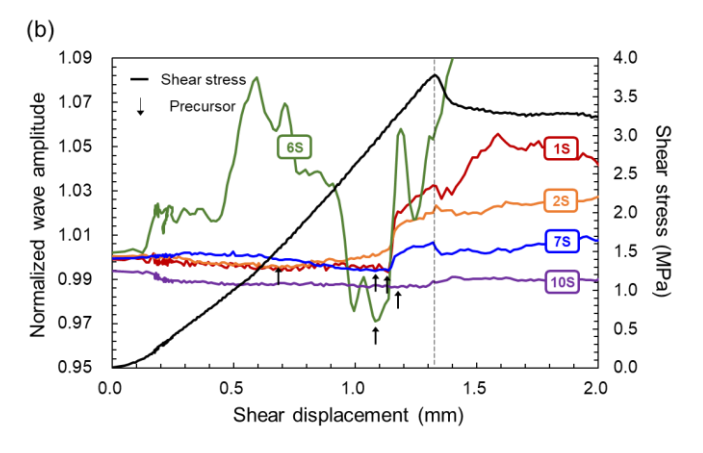
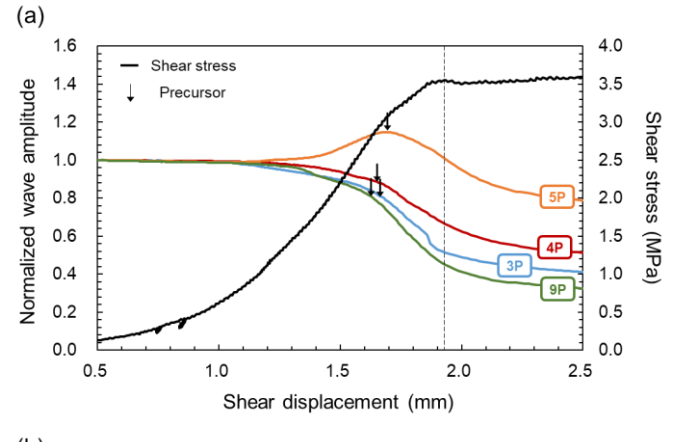


Fig. 6. Reflected wave amplitude from a rock joint under dry conditions; (a) P-waves; (b) S-waves.

3.2. Saturated Joints

Normalized transmitted wave amplitudes from a joint under saturated conditions are shown in Fig. 7, together with the shear stress – shear displacement response. In contrast to the observations for a dry joint, no distinct peak shear stress was observed. The peak friction angles of the dry and saturated joints were similar, and within experimental error: 60.6°, for the saturated and, 62.1° for the dry joint. The shear strength of the dry joint in this study was consistent with that from Hedayat et al. (2018).



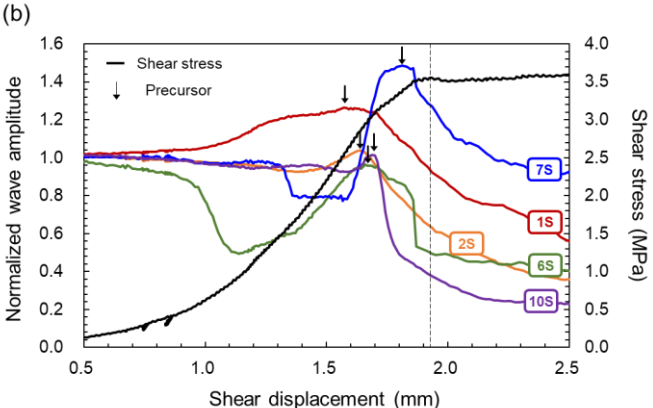
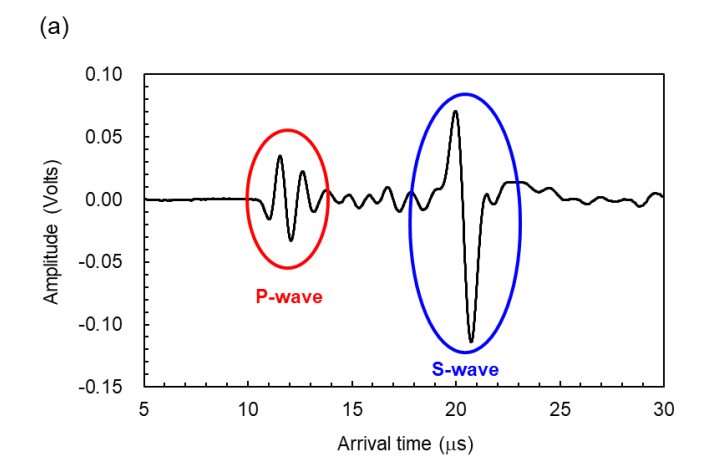


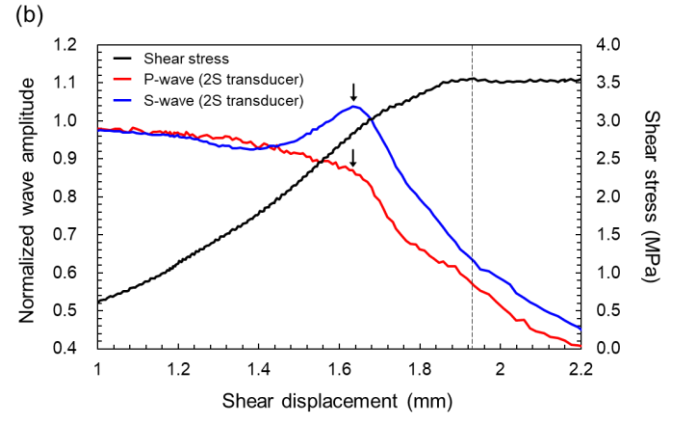
Fig. 7. Transmitted wave amplitude through a rock joint under saturated conditions: (a) P-waves; (b) S-waves.

The geophysical response of the saturated rock joint is very different from that of the dry joint. Under saturated conditions, most P-transducers did not show precursors to shear failure, but rather a monotonic decrease of amplitude with increasing shear displacement (compare Fig. 7a, for saturated conditions, with Fig. 5a for dry conditions). The data in Fig. 7(a) seems to indicate that fluid saturation prevents any increase in P-wave amplitude during the asperity interlocking, causing a continuous reduction of amplitude. However, the normalized amplitudes show changes of the rate of decrease of amplitude prior to the peak shear stress. This is an interesting observation that is discussed later. In contrast, S-waves do show a behavior similar to that of dry joints. Fig. 7(b) is a plot of the normalized amplitude of the S-waves during shear. An increase in amplitude occurs during the asperity interlocking phase, with the maxima corresponding to precursors to shear failure, followed by a continuous decrease in amplitude, even after the peak shear stress.

As mentioned, almost all the P-waves showed a continuous reduction in amplitude under saturated conditions but with distinct changes in rate at which they decrease. It is informative to explore if those rate changes are indicative of seismic precursors and how change in slope relates to the precursors detected by shear waves. Given that a full waveform captured by a S-wave transducer contains both a P-wave and a S-wave, rather than comparing P- and S-waves from different transducers, the P- and S-waves recorded by the same transducer are investigated.

Fig. 8(a) displays a 25 µs window of a signal from transducer 2S, when both the P- and S-waves are recorded. The changes in P- and S-wave amplitude are shown in Fig. 8(b). The P-wave amplitude recorded by the 2S transducer exhibits a continuous reduction in magnitude followed by a sudden change in amplitude (at a shear displacement of 1.63 mm). Fig. 8(c) is a graph of the slope of the normalized wave amplitudes in Fig. 8(b) and shows that the slope of the S-wave amplitude, at its peak, is zero. Interestingly, this coincides with the sudden change in slope of the P-wave. Fig. 9 shows the same graphs of Fig. 8, but for transducer 7S. Similar to the behavior observed with the 2S transducer, the sudden change in slope of the P-wave occurs close to the zero slope of the S-wave amplitude at its peak (Fig. 9(c)). Thus, an onset of a dramatic change in the slope of the P-wave amplitude may also be used as a seismic precursor to shear failure. However, for verification of a sudden change in the slope of the P-wave as a precursor, consistent observations are still required from additional experiments.





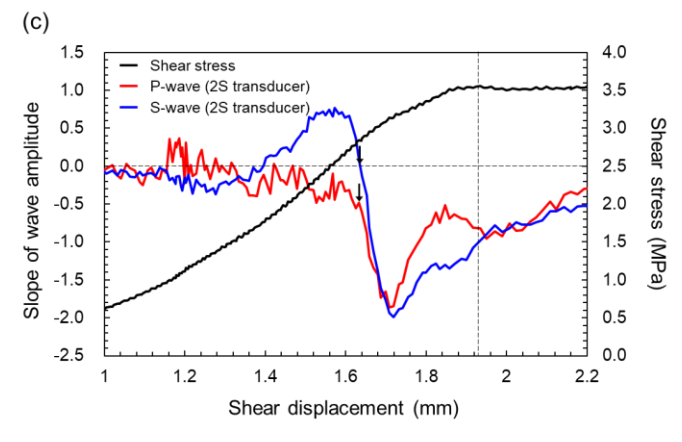
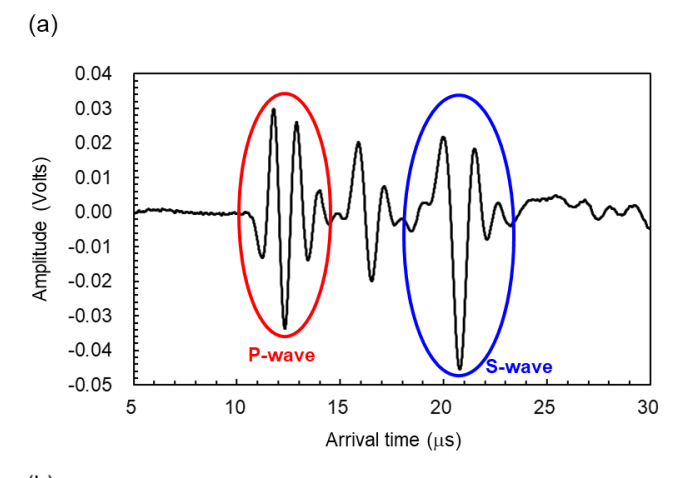
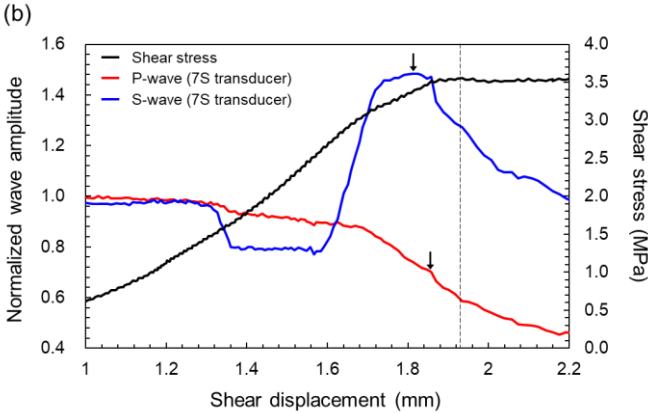


Fig. 8. Seismic wave captured by 2S transducer: (a) waveform during the time interval of $5 - 30 \mu s$; (b) Normalized P- and S-wave amplitudes; (c) Slope of the P- and S-wave amplitudes.





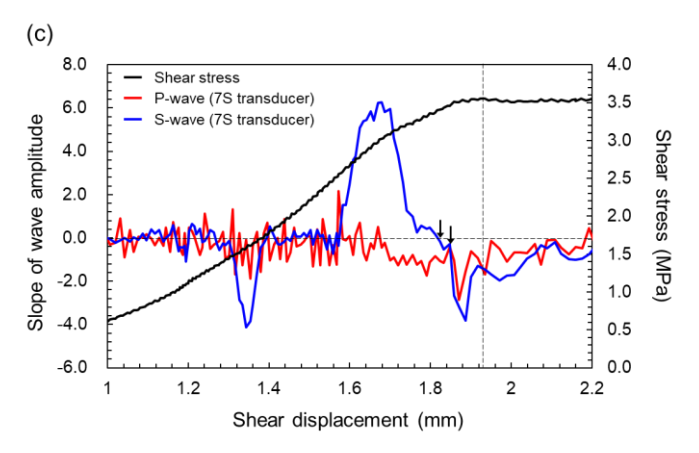
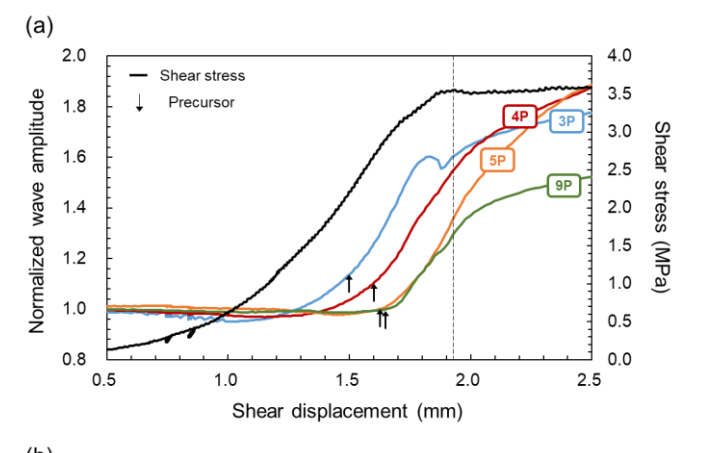


Fig. 9. Seismic wave captured by 7S transducer: (a) waveform during the time interval of $5-30 \mu s$; (b) Normalized P- and S-wave amplitudes; (c) Slope of the P- and S-wave amplitudes.

The normalized reflected amplitudes, for saturated conditions, are presented in the graph in Fig. 10. The reflected P-wave and S-wave amplitudes are shown in Fig. 10(a) and Fig. 10(b), respectively. The reflected waves indicate a continuous increase in the amplitude of the P-waves, while distinct minima in peak amplitudes of S-waves occur prior to shear failure of the saturated joint. Also, in a manner similar to that observed in the transmitted waves, a sudden change in the slope of the P-wave amplitudes may be taken as precursors to shear failure, as it occurs close to minima in peak amplitude of the S-waves.



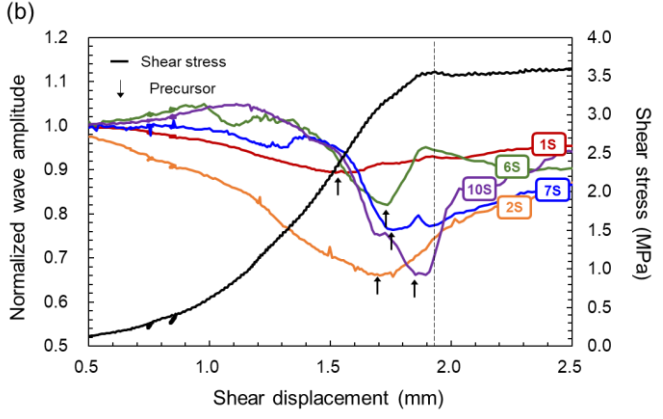


Fig. 10. Reflected wave amplitude through a rock joint under saturated conditions: (a) P-waves; (b) S-waves.

4. SUMMARY AND CONCLUSIONS

The presence of water affects the transmission and reflection of elastic waves from rock joints. For dry joints, both transmitted P- and S-waves show a maximum wave amplitude prior to shear failure. However, for saturated joints, a precursor is only observed in the S-waves amplitudes, in both transmitted and reflected waves. The tests show that P-waves, propagated through saturated rock, have a continuous decrease in amplitude. However, sudden changes in the slope of the P-waves can be taken as seismic precursors to joint shear failure. In all cases, reflected S-waves display precursors to shear failure in the form of minima of the normalized amplitude.

ACKNOWLEDGEMENTS

This research has been supported by the National Science Foundation, Geomechanics and Geotechnical Systems Program, with Award Number CMMI-1664562. The authors are grateful for this support.

REFERENCES

1. ASTM. (2016). Standard Test Method for Splitting Tensile Strength of Intact Rock Core Specimens. ASTM D3967, West Conshohocken, PA: ASTM.

- Barton, N. (1976). Rock Mechanics Review: The Shear Strength of Rock and Rock Joints. *International Journal of Rock Mechanics and Mining Sciences & Geomechanics Abstracts*, 13, 255-279.
- 3. Choi, M.-K. (2013). *Characterization of Fractures Subjected to Normal and Shear Stress*. Ph.D. Thesis, Lyles School of Civil Engineering, Purdue University. ProQuest.
- Choi, M.-K., Pyrak-Nolte, L.J. and Bobet, A. (2014). The effect of surface roughness and mixed-mode loading on the stiffness ratio Kx/Kz for fractures. *Geophysics*, 79(5), 319-331.
- El Fil, H., Bobet, A., and Pyrak-Nolte, L. J. (2019). Mechanical and Geophysical Monitoring of Slip Along Frictional Discontinuities. In *Proc. 53rd US Rock Mechanics/Geomechanics Symposium*, New York, NY. American Rock Mechanics Association.
- El Fil, H., Pyrak-Nolte, L. J., and Bobet, A. (2021). Transmitted, Reflected, and Converted Modes of Seismic Precursors to Shear Failure of Rock Discontinuities. In Proc. 55th US Rock Mechanics/Geomechanics Symposium, Houston, TX. American Rock Mechanics Association.
- Gheibi, A. and Hedayat, A. (2019). Ultrasonic precursors to shear failure of rock joints in Gosford sandstone with rough contact surfaces. In *Proc. 53rd US Rock Mechanics/Geomechanics Symposium*, New York, NY. American Rock Mechanics Association.
- 8. Gheibi, A., Li, H., and Hedayat, A. (2021). Detection of Seismic Precursors in Converted Ultrasonic Waves to Shear Failure of Natural Sandstone Rock Joints, *Rock Mechanics and Rock Engineering*, 54, 3611-3627
- 9. Han, K., Pyrak-Nolte, L. J., and Bobet, A. (2021). Experimental Investigation of Rock Saturation Determination. In *Proc. 55th US Rock Mechanics/Geomechanics Symposium*, Houston, TX. American Rock Mechanics Association.
- 10. Hedayat, A. (2013). *Mechanical and Geophysical Characterization of Damage in Rocks*. Ph.D. Thesis, Lyles School of Civil Engineering, Purdue University. ProQuest.
- 11. Hedayat, A., Pyrak-Nolte, L. J., and Bobet. A. (2014a). Multi-Modal Monitoring of Slip Along Frictional Discontinuities. *Rock Mechanics and Rock Engineering*, 47, 1575-1587.
- 12. Hedayat, A., Pyrak-Nolte, L. J., and Bobet. A. (2014b). Precursors to the shear failure of rock discontinuities. *Geophysical Research Letters*, 41(15), 5467-5475.
- Hedayat, A., Haeri, H., Hinton, J., Masoumi, H., and Spagnoli, G. (2018). Geophysical signatures of shearinduced damage and frictional processes on rock joints. *Journal of Geophysical Research: Solid Earth*, 123(2), 1143-1160.
- 14. Jaeger, J.C. and Cook N.G.W. (1979). *Fundamentals of Rock mechanics*. 3rd Edition, Chapman and Hall, London, 1979.
- 15. Li, W., Petrovitch, C., and Pyrak-Nolte, L. J. (2009). The effect of fabric-controlled layering on compressional and shear wave propagation in carbonate rock. *International Journal of the Japanese Committee for Rock Mechanics*, 4(2), 79-85.
- 16. Mesri, G., Adachi, K., and Ullrich, C. R. (1976). Pore-pressure response in rock to undrained change in all-round stress. *Geotechnique*, 26(2), 317-330.

- 17. Modiriasari, A., Bobet. A., and Pyrak-Nolte. L. J. (2017). Active seismic monitoring of crack initiation, propagation, and coalescence in rock. *Rock Mechanics and Rock Engineering*, 50(9), 2311-2325.
- 18. Nakagawa, S., Nihei, K. T., and Myer, L. R. (2000). Shear-induced conversion of seismic waves across single fractures. *International Journal of Rock Mechanics and Mining Sciences*, 37(1-2), 203-218.
- 19. Pyrak-Nolte, L.J., Myer, L. R., and Cook, N. G. (1990). Transmission of seismic waves across single natural fractures. *Journal of Geophysical Research: Solid Earth*, 95(B6), 8617-8638.
- Pyrak-Nolte, L. J., Nolte, D. D., de Pater, C. J., and Jocker, J. (2006). Monitoring propagating fracture fronts: Exploiting Fresnel seismic precursors. In *Proc. 41st U.S. Symposium on Rock Mechanics (USRMS): "50 Years of Rock Mechanics Landmarks and Future Challenges"*. Golden Rocks, Golden, Colorado. American Rock Mechanics Association.
- 21. Scuderi, M. M., Marone, C., Tinti, E., Di Stefano, G., and Collettini, C. (2016). Precursory changes in seismic velocity for the spectrum of earthquake failure modes. *Nature Geoscience*, 9, 695-700.